Design of MEBT Short Q-magnets with Large Bores using MAFIA for the JHP Proton Linac

Kazuo YOSHINO, Takao KATO, Akira UENO and Yoshishige YAMAZAKI
National Laboratory for High Energy Physics, KEK
1-1 Oho, Tsukuba-shi, Ibaraki-ken, 305, Japan

Abstract

A radio-frequency quadrupole (RFQ) linac and a drift-tube linac (DTL) are under development for the 1-GeV high-intensity proton linac of the JHP. The design of quadrupole magnets to be used in the medium-energy beam transport line (MEBT) from RFQ to DTL is described in this paper. Since the quadrupole magnets are short, being comparable to (1.4 to 2 times as long as) the bore diameter, the leakage flux along the beam axis is quite significant. Therefore, the multipole components of magnetic fields arising from the leakage flux should be minimized by choosing the pole-piece shape on the basis of the three-dimensional analysis. The integral of the field gradient along the beam axis could be flattened within 1×10^{-3} from the beam center to the bore radius.

Introduction

A 432-MHz radio-freqency quadrupole (RFQ) linac and a 432-MHz drift-tube linac (DTL) with permanent quadrupole magnets are developed for the 1 GeV high-intensity proton linac of the Japanese Hadron Project (JHP)[1,2]. The RFQ linac accelerates the H^- beams from 50 keV to 3 MeV. The medium-energy beam transport (MEBT) line from RFQ to DTL was designed by using a newly developed, multi-particle beam simulation code, in order to suppress the emittance-growth during accelerating a beam to 1GeV[3]. As shown in figure 1, the MEBT comprises eight quadrupole magnets, one energy-analyzing magnet, one buncher cavity and two gate valves. Both logitudinal and transverse emittances are measured by emittance monitors located after the analyzing magnet.

Since the longitudinal space is thus limited as seen from the figure 1, the magnets should be shortened as much as possible. On the other hand, the bore diameter of quadrupole magnets should be chosen as large as possible compared with the beam diameter in order to avoid the beam loss. Here, the calculated maximum beam diameter was about 20 mm in the MEBT, where no alignment error was included. Considering these conflicting requirements we chose a bore diameter of 35 mm, and prepared five kinds of quadrupole magnets: one of them is 50 mm-, three of them are 60 mm- and one of them 70 mm-long, depending upon their magnetic field gradients (the maximum one is 43 T/m). Since the magnets are quite short compared with the bore diameter (only 1.4 to 2 times), the multipole components of the fields can in general be increased by the large field leakage. In order to suppress the multipole components the shape of the magnetic poles was optimised on the basis of the three-dimensional analysis by using the MAFIA[4]. The results of the analysis are described in this paper. The DC power supply for these electromagnets were chosen among the commercially availble ones which are relatively inexpensive and highly reliable.

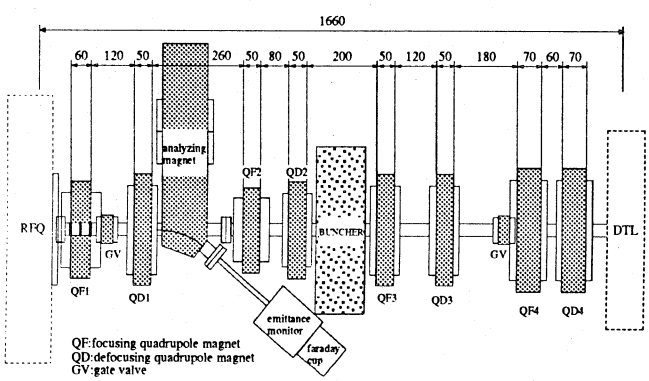

Fig. 1 Place of compornent in MEBT

Two-dimensional magnetic field analysis using POISSON

At first, we carried out two-dimensional magnetic field analysis by using POISSON[5] on the quadrupole magnet QF4 (see figure 1) for which the required field gradient is the maximum among all the magnets. The purpose of this two-dimensional analysis is to determine a rough pole-piece shape and to test if the choice of the maximum field gradient is suitable. It can be seen from figure 1 that the space to be used for the coils is most limited in between the two quadrupole magnets QF4 and QD4. The coil thicknesses should be confined within about 20 mm. We thus chose the thinnest hollow conductor with an outer dimension of 3.96 x 5.99 mm^2 and a wall thickness of 1.22 mm. The power supply was chosen in order to feed the maximum current of 300 A acceptable in this hollow conductor (the current density of 16.9 A/mm^2). The cross-sectional view of the magnet is shown in figure 2, where a pole piece forms a hyperbola given by $2xy = 17.5^2$ and the coil is wounded 21 turns per a pole. Figure 3 shows the excitation-current dependence of the field gradient G at r = 4.5 mm, where r is the displacement from the magnetic center. The dependence is shown in terms of the ratio of the field gradient G calculated by POISSON to the ideal value G_0 without saturation or flux leakage. It can be seen that

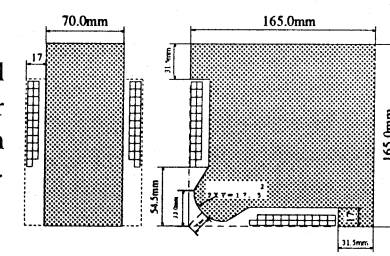

Fig.2 Cross-sectional view of the magnet for which the maximum field gradient is required.

the gradient at the design value of 43 T/m (249 A) is only by 0.7 % less than the value at 30 A, implying that no significant saturation effect appears up to the design value. Also, the field gradient is uniform within 10^{-4} from the beam axis to the bore radius of r = 17.5 mm as shown in figure 4. (The distorted distribution near the beam axis is probably due to the calculation error.) The choice of the maximum field gradient is thus justified. Even for the maximum excitation current (300 A, 49.1 T/m) the saturation effect on the field gradient distribution is small as shown in figure 4.

Three-dimensional analysis using MAFIA

As mentioned in the introduction it is necessary to carry out the three-dimensional analysis for magnets which are short compared with their bore diameters. The result of the analysis for the shortest magnet with a length of 50 mm is shown in figure 5. Since the focusing effect on the beam is represented in terms of the integral ($GL=\int_{-\infty}^{\infty} G(z)dz$) of the gradient along the beam direction, the figure shows the radial distribution of the values of GL. It can be seen that the value of a hyperbolic pole piece is decreased by 1 % at the bore radius. Note that the decrease was only 10^{-4} in the two-dimensional analysis. The flux is leaked outside the short magnet, giving rise to the increase in the multipole component. Attempts were made to improve the decrease by attaching shims to the hyperbolic pole piece, but without success. A significant improvement could be finally obtained by using the circular pole piece with shims shown in figure 6. It is seen from figure 5 that the decrease is improved to 1×10^{-3} at the bore radius. We thus decided to use the circular pole pieces with the proper shims.

In order to study the magnet-length dependence of the leakage flux in more detail we compare the longitudinal distributions of the field gradients of various magnets in figure 7. It can be seen that the gradients of all the magnets are approximately the same at the end of the pole piece (by about 20 % less), where the field gradients are normalized by the central ones. Furthermore, the gradients become 10 % of their central values at the approximately same distances from their pole-piece ends (26.2 mm, 26.5 mm and 25.5 mm for the 50-mm, 60-mm and 70-mm magnets, respectively). In other words, the leakage flux is effective in the same range for all the cases. As a result the contribution of the leakage flux to the integral GL is more significant for the shorter magnet.

In order to study the saturation effect in the three-dimensional analysis the excitaion-current dependences of the integrals GL at the beam center is shown in figure 8-A as normalized by the ideal values ($G_0L=G_0\times Magnet\ Length$). The excitation-current dependences of the filed flatnesses are also shown in figure 8-B, where the integrals GL at the bore radius are normalized by those at the radial center. It is noted in figure 8-A that the ratio GL/G_0L of the integrals of the shortest magnet is the largest (1.36), since the contribution of the leakage flux is the largest as mentioned above. For the same reason the radial flatness of the integral of the shortest magnet is the worst due to the largest multipole component. The saturation effect is observed in the three-dimensional analysis over 200 A, in particular near the design current of 250 A, more significantly than in the two-dimensional analysis. (The saturation effect is not significantly dependent upon magnet length as far as the effect is analyzed three-dimensionally.) However, the required focusing strength can be obtained by the excitation current near 200 A, since the leakage flux increases the integral GL by factors of 1.1 to 1.36. The designed values of all the magnets are listed in table 1. The design is based upon the present three-dimensional analysis. It is seen that the required excitation currents are around 200 A, where the saturation effect is relatively weak.

Conclusion

Since the space for the MEBT is limited, the quadrupole magnets must be shortened, being comparable to the bore diameter. It is thus expected that the leakage flux along the beam axis becomes significant. For this reason, the three dimensional analysis based upon the MAFIA code package is fully utilized in designing the quadrupole magnets of the MEBT. In particular the shape of the pole piece was optimized in order to obtain the tolerable radial flatness of the field gradient, since the effect of the leakage flux significantly worsened the radial flatness of the gradient in short quadrupole magnets. The integral GL of the gradient along the beam axis became radially flat within 1×10^{-3} from the beam center to the bore radius.

The saturation effects on the gradient integral GL and on its radial flatness revealed in their excitation-current dependences were more significant than those calculated by the two-dimensional analysis. However, the leakage flux along the beam axis increases the gradient integral GL compared with the ideal value G_0L by factors of 1.1 to 1.36. As a result the designed focusing strengths can be excited by the currents around 200 A, where the saturation effect is not yet significant.

The remaining problem is to investigate the interference between the magnetic fields of two neighboring magnets, since the leakage flux is found notable along the beam axis. The present calculation will be compared with the measurement of the magnetic fields.

References

1) Y. Yamazaki and M. Kihara, Proc. 1990 Linac. Conf., LANL report, LA-12004-C, 1991, pp.543-547.
2) E. Takasaki et al., "Development of the High-intensity Proton Linac for the JHP", this conference.
3) T. Kato, submitted to Proc. of the 18th Linear Accelerator Meeting in Japan, 1993 (in Japanese).
4) T. Weiland, Part. Accel. 17 (1985) 227.
5) K. Halbach et al., Part. Accel. 7(1976)213.

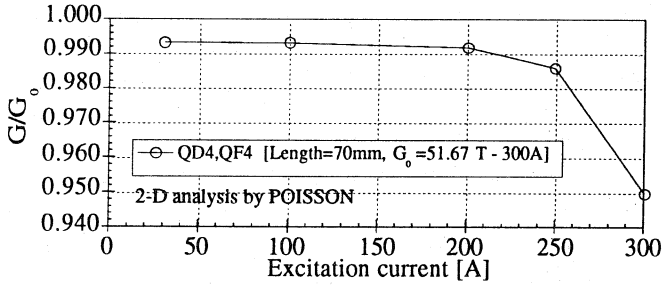

Fig.3 The excitation-current dependence of the field gradient G(r=4.5). (G_0 is the ideal value without saturation or flux leakage)

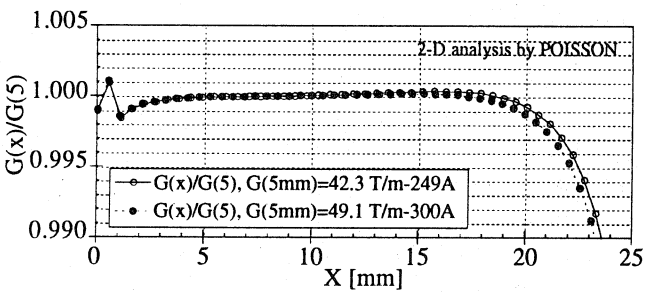

Fig.4 Radial distribution of the field gradient of the magnet for which the maximum field gradient is required.

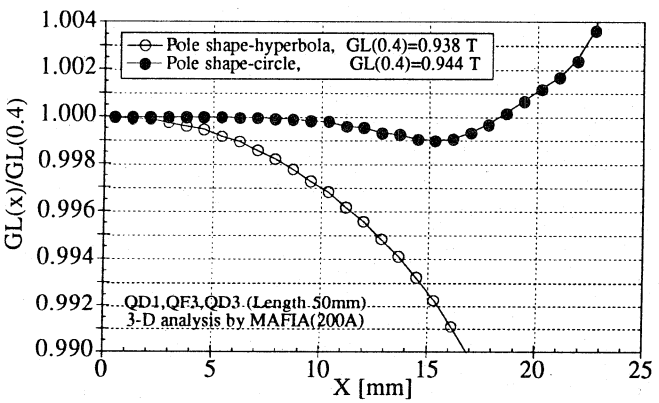

Fig.5 Radial distribution of the integral field gradient ($GL=\int_{-\infty}^{\infty} G(z)dz$) of the the shortest magnet with a length of 50 mm.

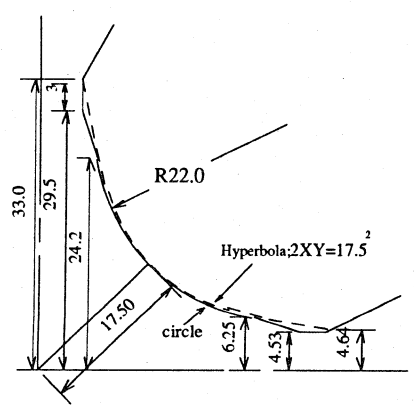

Fig.6 Cross-section view of the circular pole piece with shims.

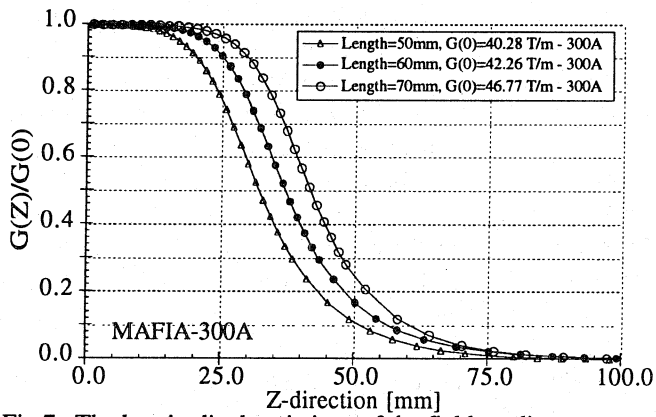

Fig.7 The longitudinal variations of the field gradients.

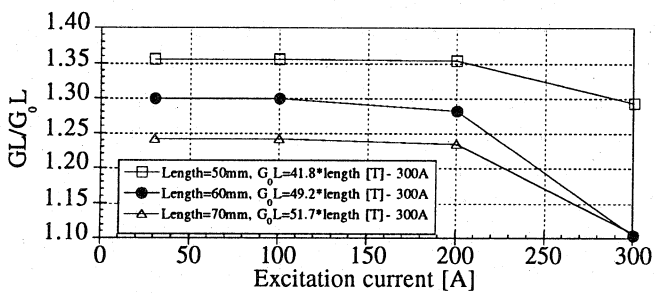

Fig.8-A The excitaion-current dependences of the integrals GL at the beam center as normalized by the ideal values ($G_0L=G_0\times Magnet\ Length$).

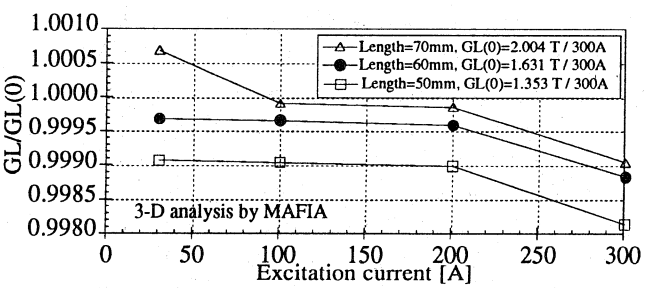

Fig.8-B The excitation-current dependences of the filed flatnesses. The integrals GL at the bore radius are normalized by those at the radial center.

		QF1	QD1,QF3,QD3	QF2	QD4,QF4	QD2
(1) Mechanical						
bore diameter	[mm]	35	35	35	35	35
core length	[mm]	60	50	50	70	50
turn number of coil	[turns/pole]	20	17	14	21	13
(2) Electric,magnetic and thermal						
current	[A]	185	177	181	202	177
field gradient	[T/m]	38.9	33.5	28.2	42.9	25.6
max field gradient(300A)	[T/m]	54.4	54.1	46.1	57.3	43.2
field effective range	[mm]	±10	±10	±10	±10	±10
resistance	[mΩ]	30.3	26.8	18.2	38.8	18.1
inductance	[mH]	60	40	17	94	14
Δ T	[℃]	13.3	12.0	8.4	18.8	8.4
flow rate of water	[liter/min]	1.88	1.88	1.88	1.88	1.88
number of water circuits		4	4	4	4	4
water pressure drop	[kg/cm²]	2.4	2.2	1.5	3.0	1.5

Table 1 Parameters of the quadrupole magnets